Preliminary result of time series analysis of InSAR observation at Semeru Volcano, Indonesia

Titi Anggono[1], Yuta Izumi[2], Estu Kriswati[1], Mohammad Hasib[1], Pakhrur Razi[3], Syuhada Syuhada[1], Nia Kurnia Praja[1], Aditya Dwi Prasetio[1], Bambang Sugiarto[1], Adam Budi Nugroho[1], Ratika Benita Nareswari[1], Febty Febriani[1], Cinantya Nirmala Dewi[1], Albertus Sulaiman[1], Wiko Setyonegoro[1]

[1]*National Research and Innovation Agency, Indonesia*
[2]*Muroran Institute of Technology, Japan*
[3]*Padang State University, Indonesia*

[a)]Corresponding author: titi.anggono@brin.go.id
[b)]yizumi@mmm.muroran-it.ac.jp
[c)]estu002@brin.go.id
[d)]moha050@brin.go.id
[e)]fhrrazi@fmipa.unp.ac.id
[f)]syuh002@brin.go.id
[g)]niak003@brin.go.id
[h)]adit015@brin.go.id
[i)]bamb059@brin.go.id
[j)]adam003@brin.go.id
[k)]rati015@brin.go.id
[l)]febt001@brin.go.id
[m)]cina001@brin.go.id
[n)]albe002@brin.go.id
[o)]wiko001@brin.go.id

Abstract. Semeru volcano is one of the most active volcanoes in Indonesia. It has been continuously active in the last several years. In early December 2021, the Semeru volcano erupted and ejected materials into the surrounding area. Such volcanic activities may lead to surface deformation in the volcanic edifice. This study investigates the Semeru volcano surface deformation from August 2020 to March 2022. InSAR observations from Sentinel-1 were used in the analysis. The time series displacement shows changes in the surface topography during the observation period. In the summit area, we observe about ~2-3 cm/year inflation rate. However, a southeastern slope from the summit seems to be deflated about ~ 6 cm/yr. From the time series of displacement, we suggest the inflation/deflation period occurred before December 2021 eruption.

INTRODUCTION

Mt. Semeru is the highest mountain in Java Island (3676 m) and one of the most active volcanoes in Indonesia. Mt. Semeru is located in East Java, Indonesia, and is surrounded by regions with dense populations, such as Malang and Lumajang. As of 2019, the population of Malang and Lumajang regency is as many as 2.6 million and 1 million, respectively [1]. Hence, the volcano becomes a concern for the government regarding its risk to the population. Semeru volcano is a stratovolcano located in the southernmost part of Semeru-Tengger volcanic complex and consists of a caldera and several cones and craters but only one of them is still active [2]. The Semeru-Tengger volcanic complex

includes Bromo-Tengger, Jambangan, Ajek-Ajek calderas, Mt. Kepolo and Mt. Mahameru-Semeru cone [3]. It was suggested that the Bromo-Tengger caldera was formed in Late Pleistocene – early Holocene [3]. Semeru volcano is located on the overlapping of Ajek-ajek and Jambangan calderas (Fig. 1). Lines of maars are visible along N-S direction through the summit. The volcano activity has been recorded since the 1800s, and the eruption has been continuously occurring since 1967. The activity not only consists of magmatic but also phreatomagmatic eruptions [3, 4]. Lava flows, for examples in 1895 and 1941 eruptions, have been recorded from the fissures or vents and reached as far as 9 km from the summit [4]. The volcano has been an active lahar producer. It was suggested that large-scale lahars (1.5 – 6 million m^3) have occurred several times [3]. Siswowidjoyo et al. [2] estimated that volume of lahars 6 million m^3 occurred in 1909 and 1981 activities on the eastern flank.

Mt. Semeru has been active for the last several years. It includes lava flows, Vulcanian and Strombolian eruptions, pyroclastic flow, lava domes, and lahars [5, 6]. Recent activities have been ongoing since 2014. Two of the latest notable eruptions occurred in early December 2000 and early December 2021. On December 1, 2000, pyroclastic flows were observed from the central lava dome with hot ashes traveled as far as 2-11 km to the southeastern flank. On December 4, 2021, a phreatomagmatic eruption and dome collapse occurred near the summit. It produced ash plumes up to 15 km in height, and pyroclastic flow into the Kobokan river causing lahar. Pyroclastic flow and lahar were observed up to 4 and 13 km, respectively, and caused significant damage to several villages surrounding the volcano. It was suggested that up to 50 fatalities were estimated due to the December 2021 eruption. Pyroclastic flow and lahar were repeatedly produced throughout December 2021 [7]. The International Charter Space and Major Disaster, which used Pleiades-1A data taken on December 9, 2021, showed dome collapse and lava flow up to 840 m from the vent (https://disasterscharter.org/image/journal/article.jpg?img_id=11947202&t=1650641080645) [8]. Since December 16, 2021, the government has raised the alert status of Semeru to Level 3 (scale 1-4).

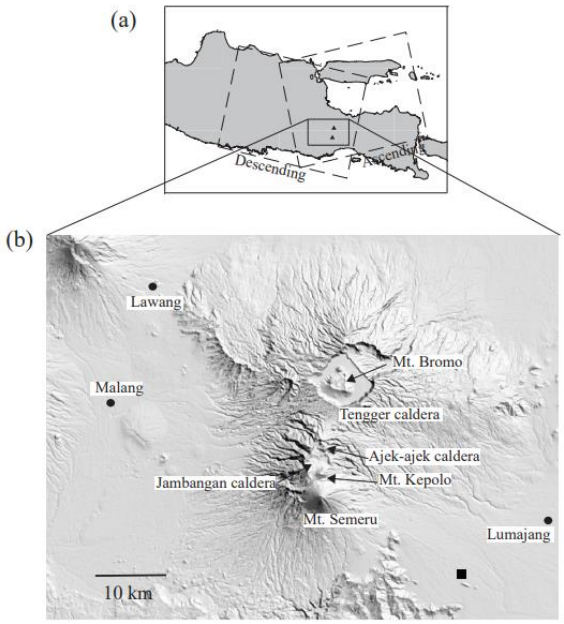

Figure 1. (a) Location of Semeru volcano, Indonesia. Swath of Sentinel-1 ascending and descending InSAR images are shown in dashed squares. (b) Semeru volcano is part of Semeru-Tengger volcanic complex. It is located at East Java, Indonesia and surrounded by cities with large population (black solid circles). Black solid square represent the reference point for deformation time series.

Recent developments in InSAR have enabled us for volcanic observation in near real time and fine resolution. The availability of free observation data from InSAR satellites such as Sentinel-1 has led to large numbers of new analysis method and field observations from volcanoes around the world. The information from InSAR measurements provides surface deformation and insight into subsurface characteristics and volcanic activity from coherence [9], and

topographic change [10]. With frequent repeat passes, scientists can monitor volcanic activities. Sigmundsson et al. [11] observed deformation at Ba´rðarbunga volcanic complex during dike emplacement in 2014. Yunjun et al. [12] measured deformation time series at the Kirishima volcanic complex using ALOS and ALOS-2 for the period of 2006 – 2019. In this study, we present about one and half year long (August 2020 – March 2022) Interferometric Synthetic Aperture Radar (InSAR) observation. We estimate the deformation time series covering the December 2021 Semeru activity.

DATA AND METHOD

We investigate the surface deformation using synthetic aperture radar (SAR) from Copernicus Sentinel-1A C-band (5.5 cm wavelength), which is operated by the European Space Agency (ESA). We use Terrain Observation by Progressive Scans (TOPS) mode for the data processing. The datasets are processed into interferograms of surface deformation projected into radar LOS. The dataset are image series from ascending and descending tracks of Sentinel-1A. The ascending SAR image covers a period of August 2, 2020 - March 13, 2022. Meanwhile, the descending SAR images covers the period of August 10, 2020 – February 13, 2022. Total number of data for ascending and descending SAR images are 49 and 42, respectively. Both ascending and descending images are processed into interferograms using InSAR Scientific Computing Environment (ISCE) software [13]. The interferograms are corrected for topography using 1 arc-second (~30 m) Shuttle Radar Topography Mission (SRTM) digital elevation model (DEM). The interferograms are filtered using Goldstein filter with a strength of 0.5. The multilooking factor is selected to be 23 × 7 for range and azimuth directions. We phase-unwrap the interferograms using minimum Statistical-Cost, Network-Flow Algorithm for Phase Unwrapping (SNAPHU) algorithm [14]. We compute interferograms up to four nearest-neighbor connections. Fig. 2 shows the interferogram network used in this study.

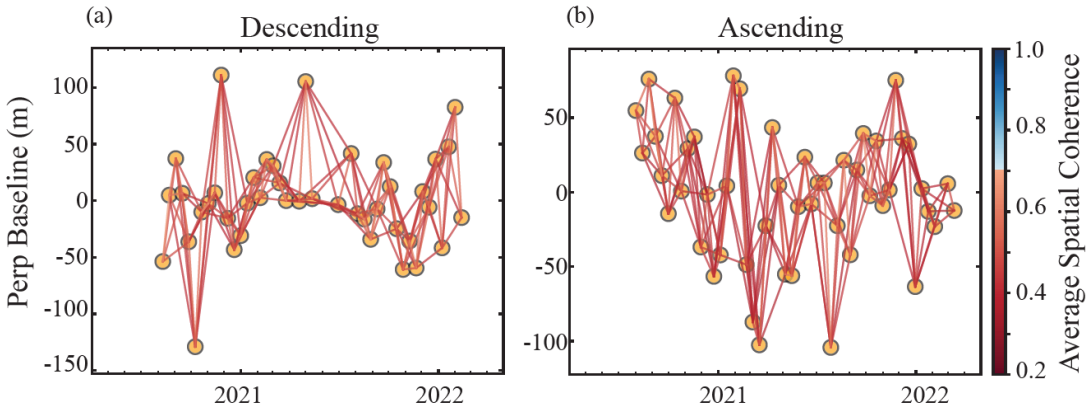

Figure 2. Interferogram network with four nearest-neighbor connections for (a) descending and (b) ascending orbits.

We apply small baseline subset (SBAS) techniques for InSAR time series analysis. The technique assumes that interferograms with a small geometric and temporal baseline maintain the coherence of the scatterers [15]. Figure 2 shows interferogram networks for both ascending and descending orbits. It is also possible to exclude SAR images with long perpendicular baselines to improve the coherence. We analyze InSAR time series analysis using Miami InSAR time series software in Python (MintPy) [16]. MintPy proposed a method to correct or exclude phase-unwrapping errors. We correct unwrapping errors by using bridging and followed by phase closure. We also select the minimum average coherence of 0.7 for a reliable measurement. To reduce tropospheric phase noise, we use an empirical linear relationship between InSAR phase delay and elevation. It was suggested that the approach may outperform correction on strong topographic variation compared to Global Atmospheric Models [16]. We estimate the topographic residual phase due to DEM error using proportionality with the perpendicular baseline.

RESULT AND DISCUSSION

The InSAR mean displacement velocities for ascending and descending tracks for period August 2020 – March 2022 are shown in Fig. 3. Using coherence threshold of 0.7, reliable pixels around the Semeru summit are limited for

descending track. We observe more reliable measurements around the Semeru summit for ascending track. Hence, we examined time series displacement using the result from the ascending track. The InSAR observation may provide high resolution of Earth's surface changes or deformation during the repeat acquisition of a satellite. This observation suffers from temporal and geometrical decorrelation, which produce phase noise. Temporal decorrelation may occur when the physical nature on the Earth's surface changes during the acquisition period, such as vegetation changes, water contents or others. Meanwhile, the geometrical decorrelation may occur due to differences in imaging geometry such as satellite position in the orbit. The occurred decorrelation or phase noise between two acquisition images can be defined as coherence, which value ranges between 0 and 1. It has been suggested that an increase in perpendicular baseline, which measure the distance between two SAR antenna, will increase decorrelation resulting in low coherence [17]. This is because the look angle changes may cause different backscattering characteristics from the study area. So, it is necessary to estimate the coherence value to have a reliable interpretation from the obtained interferograms.

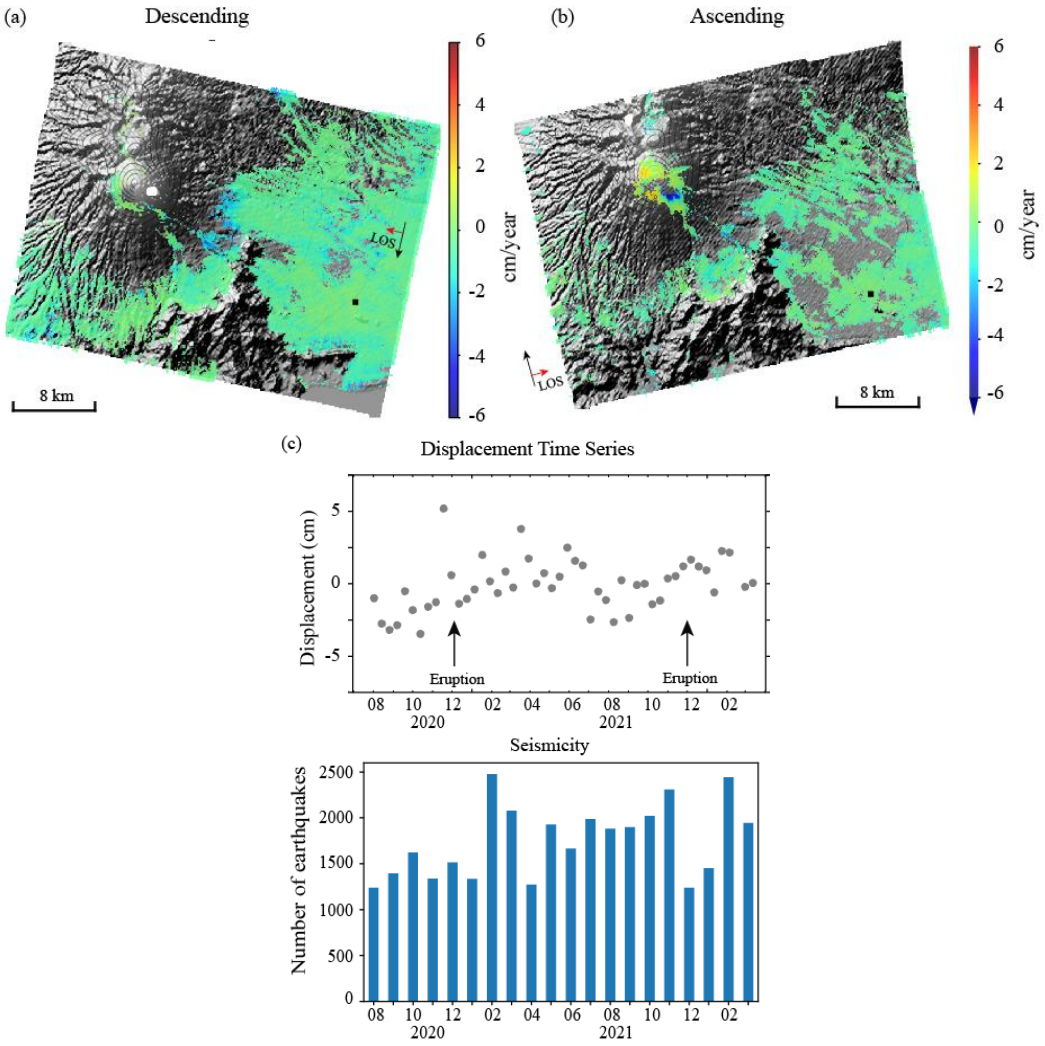

Figure 3. Deformation rate of Semeru volcano from (a) descending, (b) ascending tracks, (c) displacement time series from August 2008 to March 2022 and a monthly number of earthquakes.

In the Semeru summit area, we observe a displacement rate of about ~2-3 cm/year (Fig. 3b). In the southeastern direction from the summit, subsidence/deflation of ~ -6 cm/year is observed. Fig. 3c shows the displacement at a point in the Semeru summit (112.9238, -8.1130) from August 2020 to March 2022. We may observe three periods from the displacement time series with different trends. First, in the period of March 2020 – May 2021 we interpret as inflation period. This is due to increase displacement is observed during this period. Increase/positive displacement indicates

motion towards the satellite. Second, in the period of June – July 2021 the displacement time series shows a decrease displacement, which we interpret as deflation period. Third, for period of July – December 2021 we have positive displacement trend, which we interpret as inflation period. We compare these results with the seismicity at Semeru volcano. During the first period, we observe that there is an increase of monthly earthquakes from August 2020 to February 2021. Then the number of monthly earthquakes decreases to May – June 2021, which we interpret as coincidence with the second period from the displacement time series. The number of earthquakes increases in July – November 2021, consistent with the inflation period analyzed from the displacement. The number of earthquakes in December 2021 decreases significantly after the eruption in early December 2021. From these results, we may observe inflation/deflation period of Semeru volcanic activity from the InSAR displacement time series. However, it is necessary to discuss about possible volumetric source, which may explain the volcanic source dynamics, at Semeru volcano.

Gradual inflation often occurs before the eruption at an active volcano. When eruption occurs, it may cause rapid deflation as magma flows out and pressure is reduced [18]. An example of earthquake swarms associated with the volcanic activity is observed at Eyjafjallajökull volcano intrusive period [19, 20]. Pedersen and Sigmundsson [20] observed that the earthquake swarms began in early July 1999 and were followed by two months of low activity from mid-September to mid-November. Crustal deformation inferred from tilt and GPS was suggested starting between July – August and ending between February – May 2000. It was suggested that the deformation caused by inflating Mogi source [19]. The inflation period may extend between months and years with rates of 1 – 10 cm/year [21]. However, it is also suggested that the inflation rate > 19 cm/year is also possible [22].

CONCLUSION

We apply time series displacement analysis using InSAR observation data in the period of August 2020 – March 2021 at Semeru volcano from Sentinel-1. We estimate the displacement rate at the summit of Semeru volcano is about ~2 cm/year, and localized area in the southeastern direction from the summit experienced subsidence/deflation up to ~ -6 cm/year. From the LOS displacement time series from August 2020 – March 2022 data, we suggest inflation/deflation period occur in this period. Volumetric source may still need to be examined in the future study to understand the volcanic source dynamics generating the behavior of Semeru volcano. Longer period data may be beneficial to be investigated because the Semeru volcano has been active for several years. It is also important to include geodetic measurement (GPS) located at Semeru volcano to compare the absolute displacement obtained from the InSAR observation.

ACKNOWLEDGMENTS

We thank the European Space Agency (ESA) for providing Sentinel-1 data. The seismic data was provided by Center for Volcanology and Geological Hazard Mitigation (CVGHM). This study was supported by National Research and Innovation Agency.

REFERENCES

[1] BPS. "Jumlah Penduduk Menurut Kabupaten/Kota di Provinsi Jawa Timur (ribu), 2016 - 2019." https://batukota.bps.go.id/statictable/2020/06/08/802/jumlah-penduduk-menurut-kabupaten-kota-di-provinsi-jawa-timur-ribu-2016---2019.html (accessed July 27, 2022).

[2] S. Siswowidjoyo, U. Sudarsono, and A. Wirakusumah, *J. Asian Earth Sci.* **15**185-194 (1997).

[3] J.-C. Thouret, F. Lavigne, H. Suwa, B. Sukatja, and Surono, *Bull. Volcanol.* **70**(2) 221-244 (2007).

[4] A. Solikhin, J.-C. Thouret, A. Gupta, A. J. L. Harris, and S. C. Liew, *Geomorphology*, **138**(1) 364-379 (2012).

[5] T. Nishimura, M. Iguchi, R. Kawaguchi, Surono, M. Hendrasto, and U. Rosadi, *Bull. Volcanol.* **74**(4) 903-911 (2012).

[6] C. Gomez, F. Lavigne, D. Sri Hadmoko, and P. Wassmer, *J. Volcanol. Geotherm. Res.* **353** 102-113 (2018).

[7] Global Volcanism Program, " Report on Semeru (Indonesia)," in " Bulletin of the Global Volcanism Network," Smithsonian Institution, 2022, vol. 47.

[8] I. C. S. a. M. Disasters. "Map detailing the increase in length of the 4 December 2021 lava flow as of 9 December 2021."

https://disasterscharter.org/image/journal/article.jpg?img_id=11947202&t=1650641080645 (accessed August 13, 2022).
[9] H. R. Dietterich, M. P. Poland, D. A. Schmidt, K. V. Cashman, D. R. Sherrod, and A. T. Espinosa, *Geochem. Geophys. Geosystems* **13** Q05001 (2012).
[10] J. Kubanek, M. P. Poland, and J. Biggs, *IEEE J. Sel. Top. App. Earth Obs. Remote Sens.* **14** 3282-3302 (2021).
[11] F. Sigmundsson *et al.*, *Nature* **517**(7533) 191-195 (2015).
[12] Z. Yunjun, F. Amelung, and Y. Aoki, *Geophys. Res. Lett.* **48**(11) e2021GL092879 (2021).
[13] P. A. Rosen, E. Gurrola, G. F. Sacco, and H. Zebker, "The InSAR Scientific Computing Environment," in *9th European Conference on Synthetic Aperture Radar*, Nuremberg, Germany, 23 - 26 April 2012 2012: IEEE.
[14] C. W. Chen and H. A. Zebker, *IEEE Trans. Geosci. Remote Sens.* **40**(8) 1709-1719 (2002).
[15] P. Berardino, G. Fornaro, R. Lanari, and E. Sansosti, *IEEE Trans. Geosci. Remote Sens.* **40**(11) 2375-2383 (2002).
[16] Z. Yunjun, H. Fattahi, and F. Amelung, *Comput. Geosci.* **133** 104331 (2019).
[17] A. Pepe and F. Calò, *App. Sci.* **7** 1264 (2017).
[18] D. Dzurisin, *Rev. Geophys.* **41**(1) 1001 (2003).
[19] E. Sturkell, F. Sigmundsson, and P. Einarsson, *J. Geophys. Res.* **108**(B8) 2369 (2003).
[20] R. Pedersen and F. Sigmundsson, *Bull. Volcanol.* **68**(4) 377-393 (2005).
[21] K. G. DeGrandpre, J. D. Pesicek, Z. Lu, H. R. DeShon, and D. C. Roman, *Geochem. Geophys. Geosystems* **20**(12) 6163-6186 (2019).
[22] H. Le Mével, K. L. Feigl, L. Córdova, C. DeMets, and P. Lundgren, *Geophys. Res. Lett.* **42**(6) 6590-6598 (2015).